1

How Nature Produces Blue Color

Priscilla Simonis and Serge Berthier
Institut des Nanosciences de Paris (INSP), University Pierre et Marie Curie, Paris, France

1. Introduction

Today, blue is a very fashionable color in European countries. This has not always been the case (Pastoureau, 2000), as cultural perceptions have slowly evolved since prehistoric times. In cave paintings, white, red and black have been the only available tones and these colors remained basic for Greek and Latin cultures, where blue was neglected or even strongly devalued. The word *caeruleus*, which is often used for brightly blue species, in naming plants and insects, is etymologically related to the word *cera*, which designates wax (not to the world *caelum* – sky – as often believed): it meant first white, brown or yellow (André, 1949), before being applied to green and black, and much lately, to a range of blues. Latin and Greek philosophers were so diverted from blue that they even did not notice its presence in the rainbow: for *Anaximenes* (585-528 BC) and later for *Lucretius* (98-55 BC), the rainbow only displayed red, yellow and violet; *Aristotle* (384-322 BC) and *Epicurus* (341-270 BC) described it as red, yellow, green and violet. *Seneca* (ca. 4 BC - 65 AD) only mentioned red, orange, green, violet but, strangely, also added purple, a metameric color not found in the decomposition of white light. Later in the Middle-Ages, *Robert Grosseteste* (ca. 1175-1253) revisited the rainbow phenomenon in its book "*De Iride*" and still did not find there any blue color (Boyer, 1954). Blue emerged slowly in minds and art, only after the advent of technological breakthroughs in stained glass fabrication (as introduced in the 12th century rebuild of St Denis Basilica) and after the progressive use of blue dyes, which followed the extension of woad cultivation, all after the 13th century.

Another slow emergence of blue has been observed in the development of an efficient blue light-emitting diode. Red, yellow and green solid-state diodes appeared early after the development of the first device by Nick Holonyak Jr and S. Bevacqua in 1962, but the blue diode did not become practical until the work of Shuji Nakamura, in 1993. Since then, the blue and ultraviolet diodes have gained maturity and give rise to the emergence of powerful white sources that appear to be the future of all lightening devices.

If the blue color has been slow to emerge in human culture and technology, it was not so in nature. Blue flowers, birds, fishes, reptiles, insects, spiders, shrimps… have been observed very frequently. Blue colored structures have even been found on fossil beetles. The objective of this chapter is to discover how blue colorations are achieved in living organisms.

A classification of *natural* photonic structures is not straightforward: these structures are complex, with multiscale effects and disorder. A useful classification requires some mathematical idealization of the structures. Our scheme is based on the number of dimensions

in which we can assume a total translational invariance. One-dimensional structures are only inhomogeneous in one dimension, with, perpendicularly, complete invariance for two independent translations. These one-dimensional structures are then described as "layered". Thin films, thin film stacks and Bragg mirrors (with the repetition of identical layers) are examples of one-dimensional structures. Two-dimensional structures are totally invariant under a single direction. A straight optic fiber is a two-dimensional structure. A periodic array of parallel fibers, such as the bunch of cilia in ctenophores or the aligned melanin rods in peacock or other bird's feathers, is also a two-dimensional, as well as gratings engraved on flat surfaces. In three-dimensional structures, no direction shows total invariance under translations. This is the most general geometry for a photonic structure.

When inhomogeneous, the refractive index can be periodic, in which case the propagation acquires special features that will be examined later. A one-dimensional periodic structure is the basis for a Bragg mirror that produces well-defined reflection bands around specific frequencies. Obtaining blue colors with such a system is relatively tricky and, as will be discussed in this chapter, requires particularly thin layers in order to avoid producing a metameric purple color. Blue two-dimensional photonic crystal also requires special scatterer's spacing and specific conditions: the blue coloration of the wing feathers in the magpies is a very instructive example. Somewhat more complex, when neglecting cross-ribs, microribs and lamellae slant, the *Morpho rhetenor* ribs structure is another example of a two-dimensional photonic structure that produces a vivid blue under most directions. Gratings, as found in butterflies can also produce blue iridescence for specific grating periods. Finally, blue three-dimensional photonic crystals are observed in weevils and longhorns.

2. Tyndall diffusion

Tyndall scattering by relatively distant particles in the range 40 nm – 900 nm generally produces a bluish diffuse coloration.

2.1 Theoretical background

The elastic scattering of light by isolated particles is an important chapter of electrodynamics. The physical mechanism of light diffusion is simple: the electric field which accompanies an incident light beam penetrates and disturbs the polarizable material in the scatterer, which responds by charge oscillations. The sustained acceleration of these oscillating charges produces a reemission of light, at the same frequency, but its directional distribution is much wider than in the incident light. The distribution of the scattered light essentially depends on the polarizability of the material at the incident frequency, but also on the shape of the particle – in just the same way as the relative location of antennas influences the emission direction of radio waves.

An important parameter, for classifying the scattering mechanisms is the ratio between the scatterer's size r to the wavelength λ, $x = 2\pi r/\lambda$. For $x \ll 1$, we encounter a mechanism of diffusion called "Rayleigh scattering". This type of light redirection leads to the following distribution of intensities:

$$I = I_0 \frac{1+\cos^2\theta}{2R^2}\left(\frac{2\pi}{\lambda}\right)^4\left(\frac{n^2-1}{n^2+2}\right)^2\left(\frac{d}{2}\right)^6 \quad (1)$$

where I is the intensity scattered at an angle θ from the incident direction, R is the distance from the particle's center, n is the refractive index of the particle and d its diameter. Typically, for visible light, the diameter of the scatterer should be smaller than about 50 nm to warrant a good quantitative accuracy of the scattering. This expression was probably first derived by John William Strutt (third Baron Rayleigh), based on dimensional ("similitude") arguments (Hoeppe, 1969). Assuming that the scattering is proportional to the number of atoms in the particle – which is the atom concentration times the volume V, and inversely proportional to the distance R between the particle center and the detector used for measurement, the ratio between the scattered amplitude A and the incident amplitude A_0 can be expressed as

$$\frac{A}{A_0} \propto \frac{V}{R} \lambda^x c^y , \tag{2}$$

which should be a dimensionless quantity. The light speed c and the wavelength λ should also enter the formula because this is an optical phenomenon, but we do not yet know the exponents x and y. The right-hand side of the equation, in terms of time $[T]$ and length $[L]$, has dimensions $[L]^{2+x+y}[T]^{-y}$. For this to become dimensionless, we must have $y = 0$ and $x = -2$. This means (as the volume V is proportional to the cube of the particle diameter d)

$$\frac{I}{I_0} \propto \left(\frac{A}{A_0} \right)^2 \propto \frac{d^6}{R^2 \lambda^4} . \tag{3}$$

Much of the physics of the Rayleigh scattering is already present in this result, based on this simple reasoning. In particular, the essential point is the so-called "inverse fourth power law", stating that the scattered intensity is inversely proportional to the fourth power of the wavelength. This means that the short wavelengths in the visible white light (violet-blue) are scattered much more efficiently than the long wavelengths (orange-red). The sunlight scattered by small particles appears essentially blue because the solar spectrum contains less violet than blue and because we are less sensitive to violet than to blue.

The Irish physicist John Tyndall contributed to this question as early as in 1860. He noticed the appearance of blue scattering by a vapor of hydrochloric acid, as the particles condensed into larger size droplets and its desaturation, reaching white color, when the particles became too large. Indeed the blue Rayleigh scattering is reinforced as the volume of the scattering center is increased, and continues to do so until the particle becomes larger than the illuminating wavelength. Then, standing waves and resonances start affecting the wavelength dependence of the scattering, giving rise to a much more complex scatter color. Typically, the range of particle sizes that produce a strong blue scattering is between 50 nm to 900 nm and, for this range, where the characteristics of Rayleigh scattering are still qualitatively useful, the scattering is usually called "Tyndall scattering". For spherical particles of small, medium or large sizes, a general treatment exists: Mie scattering (Mie, 1908).

This is not quite the end, as Rayleigh, Tyndall and Mie scattering only describe the scattered intensity by a single isolated particle. When considering aggregated particles,

things also become more complicated. When the distance between the particles is much larger than the coherence length of the illuminating light, the collective scattering is incoherent, which means that the diffused intensity is merely the sum of the intensities diffused by each scattering center. The incoherent scattering by "Rayleigh particles (in the range of diameters smaller than 50 nm)" and by "Tyndall particles" (in the range 50-900 nm) can still be considered as mechanisms of "Rayleigh" or "Tyndall" scattering, respectively. If the particles are closer, we encounter a case of coherent scattering and we must add vector amplitudes with respective phases rather than intensities. The multiple scattering on nearby particles provides further opportunities for standing waves and resonances and we again lose the inverse fourth power law. The intensity and scatter directions then depend on the spatial distribution of the particles and in particular, the average distance between them.

2.2 Tyndall diffusion in nature

Tyndall scattering has long been recognized to be responsible for blue coloration of the sky (Tyndall, 1869) and the color of blue eyes (Mason, 1924). It appears when small particles or voids with dimensions of the order of the wavelength of blue light (about 500 nm) are present in the propagation medium. In that case, the small wavelengths of the incident white light will be scattered and the longer wavelengths will pass undisturbed through the medium. Thus, the red and yellow wavelengths are transmitted and the blue and violet colors are scattered by the composite medium, giving out a non-iridescent light blue diffusion spectrum.

In this phenomenon, the particle's sizes and refractive indexes control the coloration. As shown here above, the intensity of the reflected light by such a system is inversely proportional to the 4^{th} power of the wavelength. The amplitude of the reflected light and its angular distribution will depend on the particle's sizes.

For incoherent Tyndall or Rayleigh scattering to occur, it is necessary that the diffusers are separated by more than the coherence length of sunlight (about 600 nm). Under this distance, coherent interaction occurs, even if the diffusive particles are randomly arranged and one can no more talk about Tyndall or incoherent scattering. This misleading fact is at the origin of several wrong interpretations of blue coloration in animals.

In living organisms, Tyndall blue is almost always present in association with underneath pigments. The underlying pigment granules absorb the incident light that penetrate through all the structural tissue and prevent desaturation by wavelengths scattered by inner tissues. They allow structural colors to be generated with a limited number of scatterers. In most cases, the pigment granules are made of melanin (Fox, 1976) but carotenoids, antocyanins and pterins (Lee, 1991; Stavenga et al., 200; Walls, 1995) can also be present, giving rise to various coloring effects.

Since the early 20^{th} century, much work has been devoted to discovering the origin of dull blue colorations seen in animals. At first, it was common to distinguish two cases: the *iridescent* blue, synonym of coherent scattering and the *non-iridescent* blue, assumed to be incoherent Rayleigh or Tyndall scattering (Fox, 1976; Mason, 1926; Mason, 1927). At that time, the difference was based on the visual observation and not from the microscopic distances between scatterers.

It is interesting to mention that, in the twenties, Mason attributed all the non-iridescent blue colorations seen in bird feathers to Tyndall scattering but was aware that, in some insects, such coloration could arise from other phenomena (Mason 1923, Mason 1927). As new experimental and imaging techniques developed, new insights showed that blue in bird feathers could also be produced by constructive interference of light waves. Interfaces between keratin and air in the spongy medullar layer of the barbs act as coherent scatterers in that case (Prum et al., 1998; Prum et al., 1999). Blue Tyndall skins also appear in birds. For example, the extinct dodo head skin was found to be showing a diffuse blue color. This skin reveals randomly arranged, fine particles, about the size of the blue light wavelength (Parker, 2005).

Fig. 1. The male dragonfly *Orthetrum caledonicum* (Libellulidae). The blue coloration of the body comes from Tyndall scattering in a waxy layer over the black cuticle (Parker, 2000). (reproduced from GNU free documentation)

Scattered blues have early been assigned to insects. The scattering occurs in the epidermal cells beneath a transparent cuticle. In the odonate order such as aeschnids, agrionids and libelluloids (*Libellula Pulchella*, *Mesothemis Simplicicollis*, *Enallagma Cyathigerum*, *Aeshnea cyanea*, *Anax walsinghami*) the bright blue diffuse coloration on their body or wings (Mason, 1926; Parker, 2000; Parker, 2005; Veron, 1973) originates from scattering centers under the cuticle. Dragonflies (Mason, 1926) and some other adult insects can also develop a waxy bloom on the surface of their cuticle. The Tyndall effect is then produced by this waxy material and coloration can be destroyed by washing it with a wax solvent (Parker 2000): see Fig. 1.

Some butterflies have also been thought to be colored by this mechanism, such as *Papillio zalmoxis* or lycaenids (Huxley, 1976; Berthier, 2006). However, recent research shows that *coherent* interferences could also explain the various observed colors in these butterflies (Wilts et al., 2008; Prum et al., 2006). Tyndall blue has also been recorded in the cuticle of the

larvae of some tent caterpillars (Byers, 1975), due to the presence of inhomogeneous transparent cuticular filaments.

Fig. 2. The male grasshopper *Kosciuscola tristis* at 30°C (left) and 5°C (right). The blue coloration accuring at high temperature comes from Tyndall scattering (from K. D. L. Umbers, with permission, Umbers, 2011)

The male grasshopper *Kosciuscola tristis*, also called "chameleon grasshopper" has the ability to change from black to bright sky blue. It has been shown that the mechanism of this color change is completely reversible and regulated by temperature changes (Filshie et al., 1975; Umbers, 2011). It is currently admitted that the blue color arises from Tyndall scattering of light on a suspension of small granules, intensified by the underlying dark background. Intracellular granule migration can explain the color change. However, recent discussion may lead to the conclusion that coherent scattering may play a role much more important than expected (Umbers, 2011).

Tyndall scattering has also been observed in molluscs (Fox, 1976; Herring, 1994) and in nudibranch mollusks (Kawaguti & Kamishima, 1964). These are obtained by small diffusive granules displayed over a pigmentary melanophore layer. Octopus and squids are sometimes able to control the blue hue of their body patterns. This adaptive blue is achieved by varying the melanophore's grains distances in order to change the underneath absorbing screen density (Fox, 1976).

Several blue mammals skins, especially in the primates family were thought to be Rayleigh or Tyndall scattered (Fox, 1976; Price et al., 1976). However, recent research on several structurally colored mammal skins pointed out that these colorations should come from coherent scattering from quasi-ordered arrays of collagen fibers (Prum & Torres, 2004).

As far as we know, it is hard to find in nature true incoherent Tyndall scattering. Diffusive layers are often made of randomly arranged particles too close from each other to assume incoherent scattering. This condition for incoherent diffusion is often misunderstood in papers that attribute to Tyndall scattering an array of disordered particles of the size of the wavelength, whatever the distance between them.

Fig. 3. Blue skins in mammals: Male mandrill facial blue skin (left) and male vervet monkey with blue scrotum (right) (reproduced from GNU free documentation)

3. Pigmentary coloration

3.1 Theoretical background

Pigmentary coloration is based on a spectrally selective absorption of the incident white-light. For a pigment to be useful, the light which has not been absorbed must be diffused in all directions, providing the same color in all directions. This means that a sheet of material colored by absorption and diffusion will appear with roughly the same color in reflection and transmission. This contrasts structural colors obtained by interference, without absorption, where back- and forward scattering colors tend to be complementary.

The physical description of a selectively absorbing material illuminated by a single frequency needs to extend the concept of the refractive index to include refraction and absorption. A simple way to do this is, at a fixed frequency, to accept to replace its real value by a complex number $\tilde{n} = n + ik$. A frequency-dependent complex refractive index (or, equivalently) a frequency-dependent complex dielectric constant can explain the optical response of dyes in a homogeneous material. But pigments require to produce diffuse scattering and this will only take place in a random inhomogeneous material or when the absorbing material appears in the form of concentrated granules. This helps providing a distinction between dyes and pigments.

3.2 Pigmentary coloration in plants

In plants, blue coloration is quite rare. However, it can be seen in some leaves, flowers or fruits. The blue is produced by modified anthocyanin pigments. A wide variety of mechanisms for modifying anthocyanin pigments has been observed in order to get blue or violet colorations. In flowers, they form complexes with flavonoids pigments and are in solution in cellular vacuoles. In leaves, they take place in chloroplasts. The structuration of

the leave surface cells can help absorption by increasing high angle incident light to be transmitted through the leave or by focusing light in the pigmentary region. For example, in the velvet-leaved anthurium (*Anthurium warocqueanum*), the surface cells are convexly curved to focus light at some internal distance, just onto chloroplasts area (Lee, 2007).

3.3 Pigmentary coloration in animals

Pigments are very common in insects where they are responsible of almost all yellow, orange, red, brown and blacks. A blue pigmented hue is however very rare and can mainly be obtained by bile pigments such as pterobilin, phorcabilin and sarpedobilin. The two last names are coming from the species from which they were first extracted: Papilio phorcas and Graphium sarpedon (Barbier, 1990; Vuillaume & Barbier, 1969; Choussy et al., 1975).

Light induce cyclisation in bile pigments and transforms pterobilin into phorcabilin which in turn converts to sarpedobilin. In butterflies, pterobilin is widely distributed while the phorcabilin and sarpedobilin remain rare (Barbier, 1981).

Pigmented blue are mainly seen in two genera: *Papilio* (*Papilio weiskei*, *Papilio phorcas*) and *Graphium* where almost all the species contain blue pigments. In the *Graphium* species (*G. agamemnon*, *G. doson*, *G. antiphates*, *G. sarpedon*), pterobilin is responsible of the blue coloration. In the *Graphium sarpedon*, pterobilin is located in the wing membrane. Moreover, the transparent scales of the ventral side of the wing improve this blue coloration by further diffusing and polarizing light (Stavenga et al., 2010). This situation is rare among butterflies. Generally, the coloration of the wing originates from the scales covering the wing. Pigments can be embedded in the scales, absorbing part of the visible light spectrum. Alternatively or in addition, interferences can provoke structural coloration or modify pigmentary colors, as explained in the next section.

Fig. 4. Swordtail *Graphium sarpedon*. The blue coloration comes from the bile pigment sarpedobilin.

Pigmented blue is also seen in the dull blue stripes of the *Nessaea* genus (Nimphalidae). This coloration has been attributed to pterobilin (Vane-Wright, 1979).

To our knowledge, pigmented blue has not been found in mammals and in other insects. However, the presence of blue pigment remains very difficult to prove, partly because of their weak solubility. Extracting and characterizing very weakly soluble pigments is a complex task that restraints the possibilities of analysis. Moreover, determining the concentrations and localization of pigments within the tissues is still a real challenge.

Pigments in bird feathers are assumed to be present since the ages of dinosaurs. Studies on a *Sinosauropterix* (125 million years old), showed that their feathers would be filled with melanosomes and thus should appear dark (Vinther et al. 2008, Zhang et al., 2010). This work was, however, taken with cautious and discussions (Lingham-Soliar, 2011).

4. One-dimensional photonic structures

One-dimensional, planar or curved, photonic structures are frequent in nature. Insects, in particular, have frequently evolved this kind of structure for the purpose of coloration, as part of signaling or camouflage strategies. The reason may be that the process of fabrication of the outer part of a cuticle by epidermal cells, layer by layer, is compatible with the formation of such structures, even if we cannot claim at the moment that these mechanisms have been understood in all details.

Many different cases of one-dimensional photonic crystal have been seen in animalia, maybe because this is the most direct way to produce a metallic and/or iridescent color and, in this way, improve specific intra or interspecific functions. We will essentially examine two cases of physical designs: the single layer film and the Bragg mirrors.

The multilayer is the most common type of iridescent structure found in beetles and is also very common in butterflies (Kinoshita et al., 2008; Noyes et al., 2007; Parker et al., 1998). In many cases, these multilayers are composed of alternating layers of chitin and air partially filled with a chitinous compound. This produces a high/low index bilayer. Constructive interferences between light reflected by different layers produce one or several colors. The dominant reflected wavelength can be determined by the thicknesses of the layers and the average refractive index (see formula 11). The wavelengths that are not reflected are transmitted and the transmission spectrum is the exact complement of reflection if the system is considered non-absorbing. The color arising from a multilayer also varies with the angle of observation. As the reflection angle increases (starting from normal), the color shifts to lower wavelengths (blue shift).

The reflectors can be epicuticular (as in cicindelinae or in some chrysomelidae) (Kurachi et al., 2002), while others are endocuticular (Hinton, 1973).

Iridescence in bird feathers comes sometimes from 1D structure. They are located in the barbules like in satin bowerbirds *Ptilonorhynchus violaceus minor* that shows a violet to black iridescence coming from a single layer of keratin on the top of a layer of melanin (Doucet et al., 2006). In European starlings *Sturnus vulgaris*, multiple layers of keratin and melanin give a green-blue iridescence (Cuthill et al., 1999, Doucet et al., 2006).

4.1 Thin films

The single self-supported thin film and the optical overlayer covering a substrate have been known since a long time, in the planar and some other geometry. Constructive and

destructive interference of light waves in thin films (soap bubbles or oil films on water) show colorful patterns. The interference occurs between light waves reflecting off the top surface of a film with the waves multiply reflected from the bottom surface. In order to obtain a nice colored pattern, the thickness of the film has to be on the order of the wavelength of the incident light.

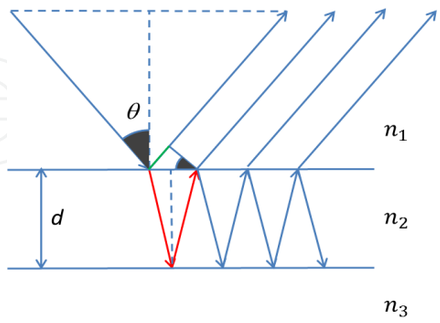

Fig. 5. Interference in a planar homogeneous slab. The phase shift between one reflected wave and its successor determine the intensity, for a given incidence angle and wavelength.

A single thin film illuminated from air reflects light at a wavelength λ as a Fabry-Pérot etalon. For a given thickness d of the film and incidence angle θ, the phase delay between the two first successively emerging rays from the multiply reflected beams is (we assume, for instance, a dense slab $n_2 > n_1$ and $n_2 > n_3$ and we name the angle of refraction inside the film: $n_2 \sin t = n_1 \sin\theta$)

$$\Delta\phi = \left\{ n_2 \frac{2\pi}{\lambda} \left(\frac{2d}{\cos t} \right) \right\} - \left\{ [\pi] + n_1 \frac{2\pi}{\lambda} (2d \tan t \sin\theta) \right\} \tag{4}$$

The first term is the phase change of the transmitted electric field wave travelling one round trip in the film before its next exit, while the last term is the progress of the reflected beam in air before joining back the other path wave. The "optional" half-wavelength phase delay (which can be written $[\pi]$ or $[-\pi]$, without consequences) occurs only when an electric wave reflects on a medium with higher refractive index. All other phase delays between successive emerging rays are the same. Maximal reflections occur when all the exiting beams are in phase, which means $\Delta\phi = m(2\pi)$, where m is an integer. This condition allows determining, under a specific incidence angle, the reinforced wavelengths, which turn out to be

$$\lambda = \frac{2n_2 d}{m + \left[\frac{1}{2}\right]} \cos t \tag{5}$$

Or, equivalently,

$$\lambda = \frac{2d\sqrt{n_2^2 - n_1^2 \sin^2\theta}}{m + \left[\frac{1}{2}\right]} \tag{6}$$

Note that, if the refractive index n_3 is larger than n_2 (itself larger than n_1), the addition of $1/2$ at the denominator must be skipped. The dependence of this dominant reflected wavelength on the incidence angle θ, which means a change of color with the angle under which the surface is viewed, is the phenomenon of iridescence, which often signals a structural color.

A typical blue color is perceived for a dominant reflected wavelength of 475 nm. Take, specifically, a thin film of thickness 200 nm and refractive index 1.5. The branch $m=0$ reflects infrared radiation, from 1470 nm under normal incidence to 1150 nm under grazing angles. The $m=1$ order extends in the visible, from 490 to 385 nm: providing short-wavelength blue coloration. The $m=2$ and higher orders are deeper in the ultraviolet.

A natural example comes from the study of the iridescent wing of a giant tropical wasp, *Megascolia procer javanensis* (Sarrazin et al., 2008). In this particular case, the wing is shown to be made of rigid structure of melanized chitin, except for an overlayer, on each side of the wing. The overlayer can be shown to act as a transparent interference thin film with a thickness of 286 nm. The refractive index of the material in this layer is not precisely known, so that its analysis requires examining the reflectance spectrum in detail, for various angles of incidence. The substrate supporting this layer is better known, as a solid mix of chitin and melanin. This mix was studied by de Albuquerque (de Albuquerque et al., 2006), including the dispersion related to melanin absorption. This absorption is strong here, as can be seen from the opacity of the wing. An adjustment of the refractive index of the overlayer allows the reflectance spectra to be fitted quite nicely at all incidence angles, and provides a value $n \approx 1.76$, which is very reasonable. The iridescence is weak: from bluish green near-normal incidence to greenish blue under a grazing incidence.

4.2 Bragg mirrors

The stacking of multiple planar layers (or "multilayers structure") is another type of structure that produces selective reflection. Among these, one important class is the periodic stack, where a group of two layers is repeated a finite number of times. This structure is also known as a Bragg mirror. When the number of periods is large (but, in practice, it does not need to be in excess of, say, 3 or 4 in the kind of structures examined here), the optical response can be approached by assuming an infinite number of periods, which can be called a one-dimensional photonic crystal. In this case, it is not very difficult to predict the dominant color that will be reflected.

In this limit, the incident frequency is conserved in all scattered waves, but not the wave vector in the stacking direction. A wave with wave number k_z will change this wave number so that its output value is a choice of any of the quantities $k_z + m(2\pi/a)$, where m is an integer and a is the period thickness:

$$k'_z = k_z + m\frac{2\pi}{a} \tag{7}$$

This means that, in a periodic multilayer stack, waves propagate normally, unless their wave vector k'_z obeys the above relation. For waves at the conserved incident frequency ω, this implies that

$$k_z = \pm\frac{\pi}{a}, \pm 2\frac{\pi}{a}, \pm 3\frac{\pi}{a}... \tag{8}$$

This corresponds to wave number values that match the so-called Brillouin-zone boundaries. For low contrasts of refractive indexes, defining an average refractive index $\overline{n}$ for the whole structure is a good starting point, taking the perturbation point of view. In this average material the following dispersion relation holds,

$$\omega = \sqrt{k_y^2 + k_z^2}\,\frac{c}{\overline{n}} \tag{9}$$

where c is the light velocity in vacuum and k_y the wave vector component parallel to the layers. This quantity is conserved across the interfaces, so that anywhere in the structure,

$$k_y = \frac{\omega}{c}\sin\theta_i\,, \tag{10}$$

where θ_i refers to the incidence angle in the incidence medium (with refractive index assumed to be 1). At the zone boundaries, the k_z and $-k_z$ modes are degenerate, but with the appearance of the refractive index contrasts, the degenerescence is lifted because of the formation of standing waves that adopt different configurations relative to high and low refractive-index regions. Then, a gap (forbidden frequencies) appears when the unperturbed dispersion curve crosses the zone boundaries, and this occurs for incident wavelengths in narrow bands centered on (m integers) (Vigneron et al., 2006)

$$\lambda = \frac{2a\sqrt{\overline{n}^2 - \sin^2\theta_i}}{m} \tag{11}$$

An incident light wave with a frequency in these ranges, impinging on the surface of this semi-infinite photonic crystal, will be totally reflected. We note that, on a photonic crystal surface, total reflection can occur under normal incidence, and also when air is the incidence medium, contrasting our usual knowledge of total reflection conditions.

In order to produce blue (say 480 nm) under normal incidence and violet under grazing incidence (say 350 nm - many living organisms have UV vision), this equation fixes the refractive index average (1.46) and the period a (162 nm). This, however, still leaves ample flexibility in choosing the actual bilayer that defines a period. These values, calculated for the first gap ($m = 1$), are easily produced with biopolymers such as chitin or keratin, with refractive indexes close to 1.56.

It is also possible to produce long-wavelength blue (say 480 nm) under normal incidence with the second gap $m = 2$ because the fundamental reflection ($m = 1$) would not appear in the visible, but in the infrared, near 960 nm. However, under larger incidences, iridescence may bring in red contribution to the spectrum, turning violet into some extraspectral metameric color in the purple range.

A good example of this structure is provided by the "blue beetle" *Hoplia coerulea*. This structure could have been classified as a two-dimensional photonic crystal, to be described later, but the optical response is in fact close to that expected for a Bragg mirror, for reasons that will become clear in a moment.

Hoplia coerulea, has evolved a cuticle bearing scales Fig. 6 (left). The inner region of these scales is structured to filter out a spectacular blue-violet iridescence on reflection (Vigneron et al., 2005). The cuticle, as seen in scanning electron microscopy is shown in Fig. 6 (right). The scales are attached by a single peripheral point to the underlying cuticle. These scales are easily removed by breaking this binding.

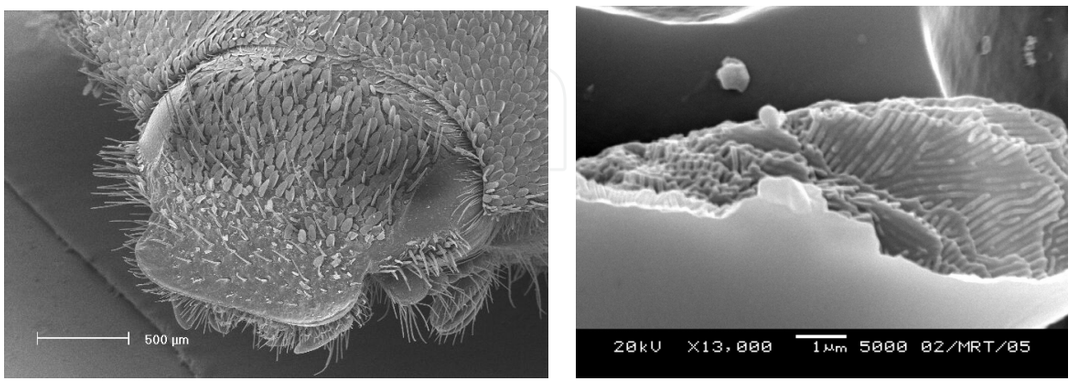

Fig. 6. *Hoplia coerulea* (right). The beetle's cuticle is covered by scales. The scales take the shape of a disk, with a diameter of about 50 µm and a thickness of 3.5 µm. These scales render a blue or violet color. The scanning electron microscope images (right) shows the coloring structure inside the scales (with permission).

The structure in each scale can be interpreted as a stack of some 20 sheets, roughly parallel to the cuticle. Each sheet is actually composed of a very thin plate of bulk chitin, bearing, on one side, a network of parallel rods with a rectangular section. The lateral corrugation associated with the rods has a period of 170 nm, just too small to produce the diffraction of light in the visible range. This acts as a zero-order grating: for visible wavelengths, the rods array appears to be a homogeneous layer, and the concept of an average refractive index is adequate. The average refractive index of the whole structure was evaluated to $\overline{n} = 1.4$ for unpolarized light near normal incidence. As the vertical period turns out to be 120 nm + 40 nm =160 nm, it fulfills perfectly the conditions described above for the production of weakly iridescent blue. The *Hoplia coerulea* structure gives some iridescence, ranging from blue to violet, and effectively behaves as a flat multilayer structure, in spite of the lateral structuring of the rods layers. This structure was recently shown to have an optical response modifiable in presence of humidity, because water can infiltrate the voids. Strangely, the structure's materials turn out to be hydrophilic (Rassart et al., 2009).

Under a crude approximation, the structure carried by the ridges of *Morpho* butterflies (for instance *M. menelaus*) can be viewed as a stack of alternating chitin and air layers, with a period of the order of 180 nm and an average refractive index well under 1.4 (Berthier et al., 2003, Berthier et al., 2006). This can explain the normal-incidence bright blue coloration and the shift of the reflected wavelength to the violet as the angle of incidence increases. This simple model has limits: it is unable to explain the off-specular variation of the scattering and the polarization effects observed in the directional reflectance pattern (Berthier, 2010).

Plants can also produce coloring multilayers for displaying a blue coloration. Examples can be found in the genus *Selaginella*, for example *S. willdenowii* and *S. uncinata* (Lee, 1997). These plants live in the understory of Central- and South-American rainforests and, strangely,

display blue on freshly grown shadowed leaves. The blue coloration arises from a one-dimensional multilayer in the moistened cellulose of outer cell walls. The refractive index of moistened cellulose is, in the average, 1.45 and the multilayer found has a period of 160 nm (two layers of different refractive indexes and equal thicknesses, 80 nm). We again find the exact conditions to provide a blue coloration with a one-dimensional photonic crystal.

5. Two-dimensional photonic structures

In two-dimensional photonic structures, one only observes a total translational invariance in one dimension, the other two dimensions being structured by refractive index inhomogeneities. We will include gratings in this category, besides fibrous photonic crystals, both of them being encountered in nature and able to select blue reflectance.

Actually, fibrous photonic crystals can be viewed as a combination of a grating and a multilayer. From the symmetry point of view, we can view a 2D photonic crystal as totally invariant in the "fibers" directions and periodic in two directions perpendicular to the fibers. Defining the surface parallel to the fibers, these two directions are adequately defined as the surface plane and the direction of the normal. The periodicity parallel to the surface produces diffraction similar to that produced by a grating, while the periodicity along the normal, deep under the surface, produces a color selection with a Bragg mirror. Being a combination of both, a 2D photonic crystal tends to be more flexible than either a grating or a Bragg mirror to produce a color such as blue. As explained below, a short-period grating will cease diffracting as its associated lateral inhomogeneity is smaller than the shortest visible wavelength. For this wavelength and larger, the grating will act as a homogeneous average material that can only generates a specular reflection. However, with a 2D photonic crystal, the "normal" periodicity can still be there to produce color selection. If, on the other extreme, the normal periodicity is constrained by weak refractive index contrasts or a tight film thickness, the Bragg mirror will not be effective, but the lateral grating can take over and still manages to produce blue. Additionally, intermediate – less easily described – mechanisms involving simultaneously cooperating diffraction and interference color selection add new channels for producing blue.

5.1 Gratings

A grating is usually a superficial structure, periodic in a single direction (say x), with a period b. The characteristic rule which describes light scattering by a grating arises from the observation that an incident wave with wave vector k_x which travels through a medium with periodicity b comes out with a series of possible wave vectors $k'_x = k_x + m(2\pi/b)$, where m is a negative, null or positive integer.

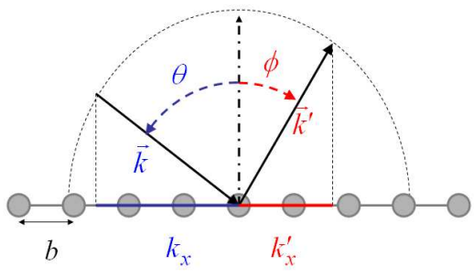

Fig. 7. Geometry of a grating, for an incident beam falling at right angle with the parallel lines.

This implies the following relationship between the incidence and emergence angles

$$\frac{\omega}{c}\sin\phi = \frac{\omega}{c}\sin\theta + m\left(2\pi/b\right) \tag{12}$$

And, more explicitly,

$$\sin\phi = \sin\theta + m\frac{\lambda}{b} \tag{13}$$

The integer m is the diffraction order. The order zero is a reflection, with emergence and incidence angles identical, with no dependence on the incidence wavelength λ. By contrast, for $m \neq 0$, the emergence angle changes with the wavelength, which means that an incidence white beam is decomposed in a colored spectrum after being scattered by the grating. Several orders may be simultaneously present, but the actual number depends on the grating period. In order to produce an acceptable emergence angle, the condition $-1 - \sin\theta \leq m\left(\lambda/b\right) \leq 1 - \sin\theta$ must be fulfilled. A given wavelength λ starts appearing in the order $m = -1$ (it will then emerge for a grazing illumination $\theta = 90°$) when

$$b = \frac{\lambda}{2} \tag{14}$$

For a larger period, the same wavelength will be observed for a range of incidence angles which contain $\theta = 90°$. This means that we actually can build gratings that produce only "blue" colors, i.e. wavelengths smaller than 490 nm (then including blue, purplish blue and violet), if the period is the rather precisely defined: $b = 245$ nm. They must be illuminated under incidence angles larger than 33°.

An example of such a grating is provided by the array of flutes found on the ridges of the scales on the butterfly *Lamprolenis nitida* (Ingram, 2008). This butterfly is special because it is equipped with two types of gratings on the same scale. One, with a large period, produces a full decomposition of the visible white light, when illuminated from the front. All colors from red to green are shown, but in this configuration, blue light is scattered with a very low intensity. The grating responsible for this coloration is shown in Fig. 8, at the tip of the arrow C. The lamellae, repeated at 700 nm spacing, are slanted in such a way as to maximize the emission in the $m = -1$ order, from red to green and to reduce the scattering in the $m = 0$ order. This can be understood as a blazed grating and the lack of blue in this coloration is the result of the precise slant angle. However, slanted in the reverse direction, the so-called "flutes" are separated by about 235 nm, not far from the period $b = 245\,nm$ mentioned above. The result is, as observed, a grating that produces only a purplish blue color, under large illumination angles.

5.2 Two-dimensional photonic crystals

Two-dimensional photonic crystals are fibers with two-dimensional periodic variations of the refractive index in the cross-section. In much the same way as with one-dimensional multilayers, the colored reflections originate from the formation of directional band gaps in the photonic band structure of these crystals. Producing blue alone from an ideal structure which fulfills these rules is difficult, because each stack of reticular plane in the two-

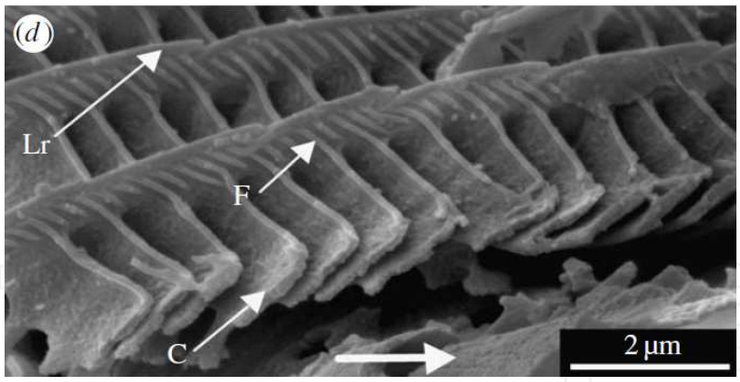

Fig. 8. The dorsal wings of male *Lamprolenis nitida* appear matt brown under incident light, normal to the wing surface, but shows various colorations under large incidences. These visual effects are due to the presence of two interspersed gratings on the scales of the rear wings. When illuminated in a postero-anterior direction and observed in backscatter, blue to violet is observed with increasing angle from the wing surface.

dimensional lattice can be considered as a Bragg mirror and the variety of values of stacking periods easily leads to the production of a wide range of colors. The coloration of fibrous organs in some marine animals, such as the Aphrodite sea mouse (Parker et al., 2001) or the Ctenophore *Beroë cucumis* (Welch et al., 2005; Welch et al., 2006), is accompanied with a broad iridescence, covering a spectral range from red to far in the ultraviolet. The high refractive index of water, compared to air, partly explains the iridescence richness, but in both cases, the structure can be viewed as a bunch of parallel fibers and a simple two-dimensional photonic crystal. Nature, however has found unexpected ways to produce blue coloration from these fibrous structures and we will give here an account of the way a bird such as the magpie (*Pica pica*) (Vigneron et al., 2006a; Lee, 2010) produces the blue reflection on some of their wing feathers.

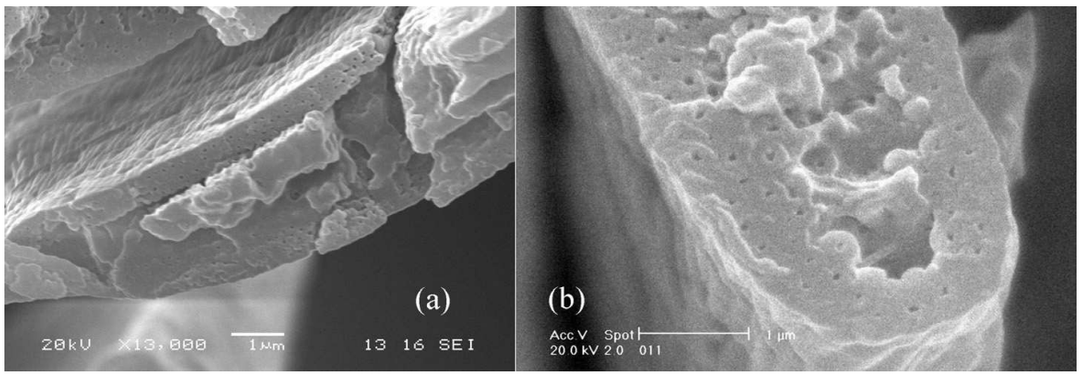

Fig. 9. The coloring structure in the tail (a) and wing (b) feather of the common magpie (*Pica pica*). The structure is formed by cylindrical melanine bars distributed to form a hexagonal two-dimensional lattice in the cortex of the barbules. The scattering centers are thin cylindrical cavities in the melanine granules and the color is related to the distance between these centers. The green color on the tail depends on the distance between the granules centers, 180 nm. Strangely, the blue photonic crystal has a larger lattice parameter (270 nm) : the coloration is controlled by a "second gap", at high frequency.

Many (but not all) birds show structural coloration at the level of the feather's barbules. A feather is rigidified by a rachis, an array of barbs attached to the rachis, and an array of barbules attached to the barb. The barbules have the topology of a sack, with an envelope (a hard cortex) containing a medullar medium. As in the Peacock's feathers (Zi et al., 2003), the coloring structure on the blue feathers of the magpie lies on the barbule's cortex. It is constituted of elongated melanine cylinders, disposed parallel to each other with the symmetry of a two-dimensional triangular lattice. These cylinders are the scatterers that produce the coherent reflection in the blue. Strangely, the distance between these scatterers is 270 nm, much too large to explain the blue coloration. In fact, simulation shows that such a fibrous crystal should produce a fundamental gap in the near infrared, and a blue scattering as a "harmonic" of this gap. Indeed, a second band of forbidden propagation exists at higher frequency. At this frequency, the diffraction is less dispersive and the blue coloration produced is relatively saturated. The coloration hue could also be spoiled by the addition of red, arising from the line width of the fundamental reflection in the infrared, producing an extraspectral purple. This is not the case: the structured cortex is thin enough to avoid producing long-wavelengths resonances and the result is a dark blue color, easily visible under a bright sunshine.

6. Three-dimensional photonic crystals

Three-dimensional photonic crystals are also encountered in nature, especially in butterflies, weevils and longhorns. In view the very high diversity of living organisms and the frequency of structural colors, it can be speculated that other families of insects will soon reveal a similar evolution. Three-dimensional photonic crystals are periodic in all three dimensions of space. Illuminated by white light in a well-defined direction, an ideal structure produces several colored beams, each of them corresponding to a stack of reticular planes with its appropriate spacing. A good example of the visual effect produced by an ideal photonic crystal is provided by the so-called Brazilian "diamond" weevil, which displays a green color when viewed from a distance, but under an optical microscope, shows individual scales with a variety of very saturated (pure) colors. Most other weevils and longhorns show less iridescence, and this is usually explained in term of orientation disorder: natural three-dimensional photonic crystals most often appear under the form of photonic polycrystals, with well-defined domains bringing short-range order and long-range orientation disorder.

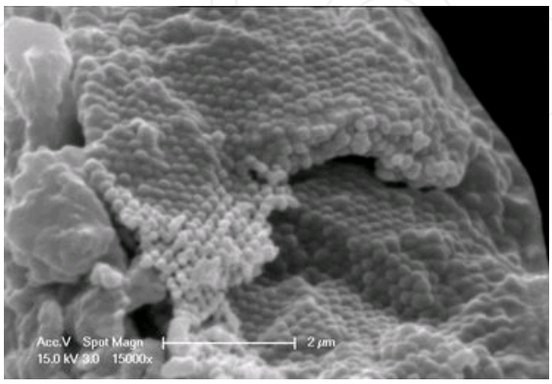

Fig. 10. The internal structure of a scale on a blue area from the cuticle of the weevil *Eupholus schoenherri*. The structure, with a face-centered cubic symmetry, can be described as an "opal" structure.

Blue weevils are frequent, in particular in the *Eupholus* genus, as *E. loriai* (completely blue) or *E. bennetti*, *E. magnificus* or *E. schoenherri* (partially blue). At the moment, the structures that produce this blue colors can be described as a photonic polycrystal with grains locally organized in a face-centered cubic symmetry. A typical "blue" structure from a weevil is shown in Fig. 10, which shows a scale from a blue area on an elytron of *Eupholus schoenherri*. The same kind of structure has been encountered in a previous work (Parker et al., 2003) for a different weevil displaying green spots. This structure is generally referred to as an "opal" structure, making a parallel with the assembly of monodispersed spheres constituting the iridescent stone. The present photonic structure is also an arrangement of non-absorbing spheres but the constituting material is a chitinous compound, with a refractive index of the order of 1.6. In order to produce short-wavelength photonic gaps, the size of the spheres is kept small and the compactness is maximized. In such a structure, the light scatterers are effectively the tiny air-filled interstices left between the spheres, not easily seen in electron microscopy images. In weevils however, the "inverse opal" structure like the one shown in Fig. 11 is the most common case. This structure corresponds to an arrangement of spherical hollows in a chitinous matrix.

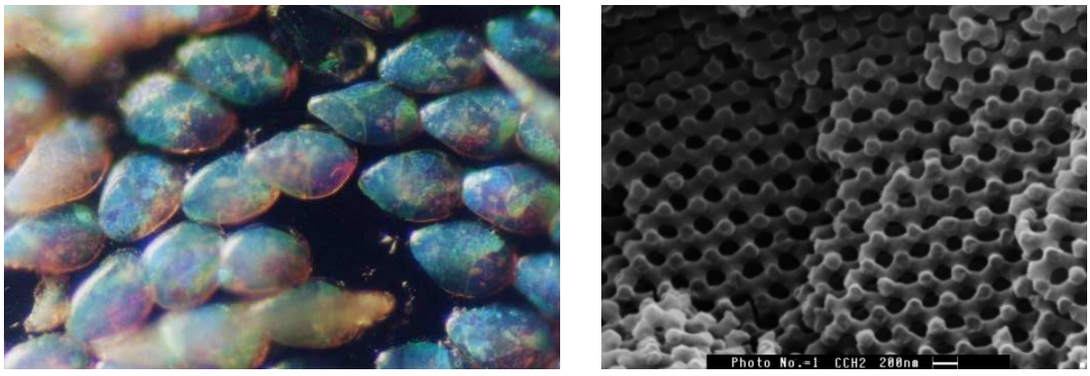

Fig. 11. Optical microscope view of the blue scales of the weevil *Cyphus hancoki*. The different colors correspond to different crystal grains (left). On the right, electron microscope image of one grain. The 3D array of spherical hollows is described as an "inverse opal" structure (Berthier, 2006).

A blue longhorn, with a three-dimensional photonic-crystal structure has also been described (Simonis et al., 2011). *Pseudomyagrus waterhousei* shows a slightly desaturated purplish blue color. These colorations arise from a dense layer of droplet-shaped scales covering the dorsal parts of the cuticle. These colors are caused by structural interferences and produced by an aggregate of internally ordered photonic-crystal grains. As in the weevils' case, the structure is built with spherical diffusion centers arranged according to a face-centered cubic symmetry. Domains are also present, with long-range orientation disorder, a complex structure which partly explains the lack of iridescence in the visual effect, in spite of a structural coloration. Theoretical considerations suggests that the contents of the observed reflectance dominantly arise from photonic crystallites with (111) reticular plane parallel to the cuticle surface. Another source of disorder lies in the observation that, in this structure, internally ordered photonic crystal grains can be separated by regions of amorphous arrangement, with spheres diameters varying over a rather wide range, from 170 to 300 nm in diameter. Here also, the short-wavelength blue

coloration is reached by increase of the structure compactness, with the production of spheres with an average diameter of 212 nm, arranged in a compact cubic structure.

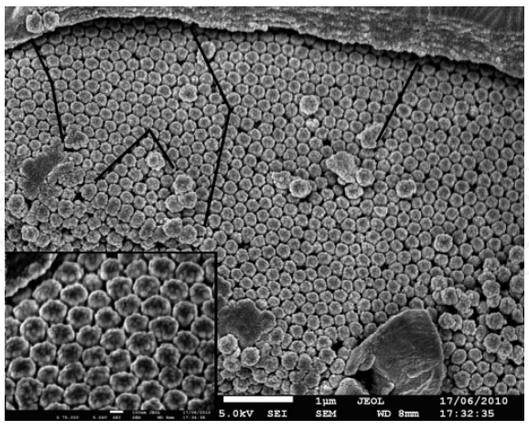

Fig. 12. The array of spherical centers found in scales of the Malaysian longhorn *Pseudomyagrus waterhousei*. The compactness of the structure leads to the production of short-wavelength scattering, providing a slightly desaturated blue-violet color.

7. Conclusion

This brief survey of the production of blue color on living organisms shows that all broad categories of structural mechanisms can be put to use to produce short-wavelengths scattering. We have seen that all structures known to be at the root of a structural coloration in nature (Vigneron & Simonis, 2010) can actually provide a blue coloration. Each device has its own rules for providing scattering solely on the short-wavelength end of the visible spectrum.

This particular objective is not always easy and often requires a multiscale solution. For living organisms that has undergone evolution over many million years, this is not a problem: the "modification-selection" algorithm, which is the engine of the past and present biodiversity, has no reluctance for complexity. Even if the range of refractive indexes in biologically prepared materials is rather narrow (typically 1.3 to 1.8), complexity in geometrical structure can provide a very wide range of functions that turn out to be an advantage for species population increase.

We do not always know what can be the biological advantage of producing blue. We understand that a male metallic blue *Morpho* can be seen from far away, which is an advantage for accelerating productive mates encounters. But the answer is less obvious for the formation of iridescent blue plants, as blue is one of the spectral components of the light captured by chlorophyll molecules to achieve photosynthesis. While an answer to the physical "how" question - referring to a description of the production mechanisms - is relatively easy, an answer to the biological "why" question is far less obvious.

8. Acknowledgment

Priscilla Simonis, on leave from the University of Namur, Belgium, acknowledges the hospitality of the "Institut des Nanosciences de Paris", Université Pierre et Marie Curie – Paris 6, where this work was carried out.

9. References

Andre, J. (1949) *Etude sur les termes de couleurs dans la langue latine*, Librairie C. Klincksieck, Paris

Barbier, M. (1981) The status of blue-green bile pigments of butterfiles, and their phototransformations, *Experientia* 37, pp1060-1062

Barbier, M. (1990) A new sarpedobilin-containing butterfly - *Papilio-Graphium-stresemani-stresemani* and its bioecological situation within the species, *J. Chem. Ecol*. 16, pp 743-748

Berthier, S., Charron, E. & Da Silva, A. (2003) Determination of the cuticle index of the scales of the iridescent butterfly Morpho Menelaus, *Opt. Comm.* 228, pp 349-356

Berthier, S. (2006) *Iridescences: the physical colors of insects*. In Springer New York, ISBN: 978-0387341194

Berthier, S., Charron, E. & Boulenguez, J. (2006) Morphological structure and optical properties of the wings of Morphidae, *Ins. Sci.* 13, pp 145-157

Berthier, S. (2010) *Photonique des Morphos (French Edition)*, Springer; 1st Edition, ISBN-13: 978-2287094071

Boyer, C.B. (1954) Robert Grosseteste on the rainbow, *Osiris* 11, 247-258

Byers, J. R. (1975) Tyndall blue and surface white of tent carterpillars, Malacosoma spp. *J. Insect. Phys.* 21 pp 401-415

Choussy, M., Barbier, M. & Vuillaume, M. (1975) Biosynthesis of phorcabilin, a blue bile pigment from *Actias-Selene* (Lepidoptera,Aattacidae), *Biochimie* 57, pp 369-373

Cuthill, I. C., Bennett, A. T. D., Partride, J. C. & Maier, E. J. (1999) Plumage reflectance & the objective assessment of avian sexual dichromatism *Am. Nat*. 53, pp 183-200

De Albuquerque, J., Giacomantonio, C., White, A. & Meredith, P. (2006) Study of optical properties of electropolymerized melanin films by photopyroelectric spectroscopy *Eur. Biophys. J.* 35, 190

Doucet, S. M., Shawkey, M. D., Hill, G. E. & Montgomerie, R. (2006) Iridescent plumage in satin bowerbirds: structure, mechanisms and nanostructural predictors of individual variation in colour *J. Exp. Biol* 209, pp380-390

Filshie B. K., Day M. F. & Mercer E. H. (1975) Colour and colour change in the grasshopper, Kosciuscola tristis *J. Insect Phys.* 21 pp 1763-1770

Fox, D. L. (1976) *Animal Biochromes and Structural colors*, University of California Press, ISBN 978-0520023475, Berkeley, CA

Herring, P. J (1994) Reflective systems in aquatic animals Comput. *Biochem.Physiol*. 109A pp 513-546

Hinton, H. E. (1973) Some recent work on the colours of insects and their likely significance *Proc. Br. Ent. Nat. Hist. Soc.* 6, pp 43-54

Hoeppe, G. (1969) *Why the sky is blue: discovering the color of life*, Princeton University Press, ISBN 0-691-12453-1

Huxley, J. (1976) The coloration of Papilio zalmoxis and P. antimachus and the discovery of Tyndall blue in butterflies, *Proc. R. Soc. Lond. B* 193 pp441-453

Ingram, A. L, Lousse, V., Parker A. R. & Vigneron, J.P. (2008) Dual gratings interspersed on a single butterfly scale, *J. R. Soc. Interface*, 5, 1387-1390

Kawaguti, S. & Kamishima, Y. (1964) Electron microscopic study on the iridophores of opisthobranchiate mollusks *Biol. J. Okayama Univ.* 10, pp 83-91

Kinoshita, S., Yoshioka, S. & Miyazaki, J. (2008) The physics of structural colors, *Rep. Prog. Phys.* 71, 30 pp, 076401

Kurachi, M., Takaku, Y., Komiya, Y. & Hariyama, Y. (2002) The origin of extensive colour polymorphism in Plateumaris sericea (Chrysomelidae, Coleoptera) *Naturwissenschaften* 89, pp 295–298

Lee, D. W. (1991) Ultrastructural basis and function of iridescent blue colour of fruits in Elaeocarpus, *Nature* 349, pp 260-262

Lee, D.W. (1997) Iridescent blue plants, *Am. Sci.* 85, 56-63

Lee, D.W. (2007) *Nature's Palette: the Science of Plant Color*, The University of Chicago Press, USA, ISBN: 9780226470528

Lee, E., Lee, H., Kimura, J. and Sugita, S. (2010) Feather Microstructure of the Black-Billed Magpie (Pica pica sericea) and Jungle Crow (Corvus macrorhynchos), J. Vet. Med. Sci. 72(8): 1047–1050

Lingham-Soliar, T. (2011) The evolution of the feather: Sinosauropteryx, a colourful tail, *J. Ornithol.* 152, pp 567-577

Mason, C. W. (1923) Structural colours of feathers I, *J. Phys. Chem* 27, pp 201-251

Mason, C. W. (1924) Blue eyes, *J. Phys. Chem*. 28, pp498-501

Mason, C. W. (1926) Structural colours of insects I, *J. Phys. Chem* 30, pp 383-395

Mason, C. W. (1927) Structural colours of insects II, *J. Phys. Chem* 31, pp 321-354

Mie, G. (1908) Beiträge zur Optik trüber Medien, speziell kolloidaler Metallösungen *Ann. Phys.*, Lpz. 25, pp. 377–445

Myiamoto, A & Kosaku, A. (2002) Cuticular Microstructures and Their Relationship to Structural Color in the Shieldbug Poecilocoris lewisi Distant, *Forma* 17 pp 155-167

Noyes, J. A., Vukusic, P. & Hooper, I. R. (2007) Experimental method for reliably establishing the refractive index of buprestid beetle exocuticle, *Opt. Express* 15, pp 4351-4358

Parker, A. R., Mc Kenzie, D. R. & Large, C. J. (1998) Multilayer reflectors in animals using green and gold beetles as contrasting examples *J. Exp. Biol*. 201, pp 1307-1313

Parker, A. R. (2000) 515 million years of structural colour *J. Opt. A* 2 pp R15-R28

Parker, A. R. (2001) et al., Photonic engineering - Aphrodite's iridescence *Nature* 409, 36

Parker, A. R., Welch, V.L., Driver D. & Martini N. (2003) Structural colour: Opal analogue discovered in a weevil, *Nature* 426, 786-787

Parker, A. R. (2005) A geological history of reflecting optics, *J. Roy. Soc. Interface* 2, pp 1-17

Pastoureau M. (2000) *Bleu, histoire d'une couleur*, Editions du Seuil, ISBN 978-2-02-086991-1

Price, J. S., Burton, J. L., Shuster, S. & Wolff, K. (1976) Control of scrotal color in vervet monkey, *J. Med. Primat*. 5, pp 296-304

Prum, R. O., Torres, R. H., Williamson, S. & Dyck, J. (1998) Constructive interference of light by blue feather barbs *Nature* 396, pp 28-29.

Prum, R. O., Torres, R., Williamson, S. & Dyck J. (1999) Two-dimensional Fourier analysis of the spongy medullary keratin of structurally coloured feather barbs *Proc. R. Soc. Lond. B* 266, pp 13-22

Prum, R. O. & Torres, R. H. (2004) Structural colouration of mammalian skin: convergent evolution of coherently scattering dermal collagen arrays, *J. Exp. Biol.* 207, pp 2157-2172

Prum, R. O., Quinn, T. & Torres, R. H. (2006) Anatomically diverse butterfly scales all produce structural colours by coherent scattering *J. Exp. Biol* 209, pp 748-765

Rassart, M., Simonis, P., Bay, A., Deparis, O. & Vigneron, J.P. (2009) Scale coloration change following water absorption in the beetle Hoplia coerulea (Coleoptera), *Phys. Rev. E* 80, 031910

Sarrazin, M., Vigneron, J.P., Welch, V. & Rassart, M. (2008) Nanomorphology of the blue iridescent wings of a giant tropical wasp Megascolia procer javanensis (Hymenoptera), *Phys. Rev. E* 78, 051902.

Simonis, P. & Vigneron, J.P. (2011) Structural color produced by a three-dimensional photonic polycrystal in the scales of a longhorn beetle: *Pseudomyagrus waterhousei* (Coleoptera: Cerambicidae), *Phys. Rev. E* 83, 011908

Stavenga, D. G., Stowe, S., Siebke, K., Zeil, J. & Arikawa, K. (2004) Butterfly wing colours: scale beads make white pierid wings brighter, *Proc. R. Soc. Lond. B* 271 pp1577-1584

Stavenga, D. G., Giraldo, M. A. & Leertouwer, H. L. (2010) Butterfly wing colors: glass scales of *Graphium sarpedon* cause polarized iridescence and enhance blue/green pigment coloration of the wing membrane, *J. Exp. Biol*. 213, pp 1731-1739

Tyndall, (1869) On the blue colour of the sky, the polarization of skylight, and on the polarization of light by cloudy matter generally, *Proc. Roy. Soc. London*. 17, pp 223-233

Umbers, K. D. L. (2011) Cues for colour change in the chameleon grasshopper (Kosciuscola tristis) *J Insect Physiol*. 57, pp 1198-1204

Verron, J. E. N. (1973) Physiological control of the chromatophores of Austrolestes annulosus (Odonata), *J. Insect. Phys*. 19, pp 1689-1693

Vigneron, J.P., Colomer, J.F., Vigneron, N. & Lousse V. (2005) Natural layer-by-layer photonic structure in the squamae of Hoplia coerulea (Coleoptera), *Phys. Rev. E* 72, 061904

Vigneron, J.P. & Virginie Lousse, V. (2006) Variation of a photonic crystal color with the Miller indices of the exposed surface, *Proc. SPIE* 6128, 61281G

Vigneron, J.P., Colomer, J.F. Rassart, M., Ingram, A.L. & Lousse V. (2006a) Structural origin of the colored reflections from the black-billed magpie feather, *Phys. Rev. E* 73, 021914

Vigneron J.P. & Simonis P. (2010) Structural Colours, in Jérôme Casas and Stephen J. Simpson, editors: *Advances in Insect Physiology*, 38, pp. 181-218, Academic Press (Burlington) , ISBN: 978-0-12-381389-3

Vane-Wright, R. I. (1979) The coloration, identification and phylogeny of Nessaea butterflies (Lepidoptera: Nymphalidae) *Bull. Brit. Mus. Nat. Hist. Entomol*. 38, pp 27-56

Vinther, J., Briggs, D. E. G., Prum, R. O. & Saranathan, V. (2008) The colour of fossils feathers *Biol. Lett*. 4, pp 522-525

Vuillaume, M. & Barbier, M., (1969) Tetrapyrrole pigments of lepidoptera, *C. R. Acad. Sci. Paris* 268, pp 2286-&

Walls, J. (1995) *Fantastic Frogs* T.F.H. Publications, Neptune City, NJ ISSN 978-0793801312

Welch, V. L., Vigneron J. P. & Parker A. R. (2005) The cause of colouration in the ctenophore Beroë cucumis, *Current Biology*, 15 pp R985-R986 Supplement

Welch, V. L., Vigneron J. P., Parker A. R & Lousse V. (2006) Optical properties of the iridescent organ of the comb-jellyfish Beroe cucumis (Ctenophora), *Phys. Rev. E* 73, 041916

Wilts, B. D, Leertouwer, H. L & Stavenga, D. G. (2008) *J. Roy. Soc. Interface* 6, pp s185-s192

Zhang, F., Kearns, S. L., Orr, P. J., Benton M. J., Zhou, Z., Johnson D., Xu, X. & Wang, X. (2010) Fossilized melanosomes and the colour of Cretaceous dinosaurs and birds, *Nature* 463, pp 1075-1078

Zi, J., Yu, X., Li, Y., Hu, X., Xu, C., Wang, X., Liu, X. & Fu, R. (2003) Coloration strategies in peacock feathers *Proc. Nat. Acad. Sci. USA* 100, pp 12576-12578

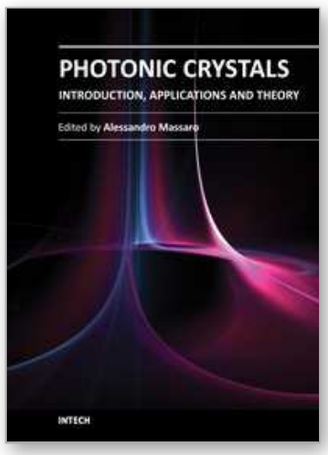

Photonic Crystals - Introduction, Applications and Theory
Edited by Dr. Alessandro Massaro

ISBN 978-953-51-0431-5
Hard cover, 344 pages
Publisher InTech
Published online 30, March, 2012
Published in print edition March, 2012

The first volume of the book concerns the introduction of photonic crystals and applications including design and modeling aspects. Photonic crystals are attractive optical materials for controlling and manipulating the flow of light. In particular, photonic crystals are of great interest for both fundamental and applied research, and the two dimensional ones are beginning to find commercial applications such as optical logic devices, micro electro-mechanical systems (MEMS), sensors. The first commercial products involving two-dimensionally periodic photonic crystals are already available in the form of photonic-crystal fibers, which use a microscale structure to confine light with radically different characteristics compared to conventional optical fiber for applications in nonlinear devices and guiding wavelengths. The goal of the first volume is to provide an overview about the listed issues.

INTECH
open science | open minds

InTech Europe
University Campus STeP Ri
Slavka Krautzeka 83/A
51000 Rijeka, Croatia
Phone: +385 (51) 770 447
Fax: +385 (51) 686 166
www.intechopen.com

InTech China
Unit 405, Office Block, Hotel Equatorial Shanghai
No.65, Yan An Road (West), Shanghai, 200040, China
中国上海市延安西路65号上海国际贵都大饭店办公楼405单元
Phone: +86-21-62489820
Fax: +86-21-62489821

IntechOpen